

# Numerical Simulation of Devolution and Evolution of Steam-Water Two-Phase Zone in a Fractured Geothermal Reservoir at Ogiri, Japan

Yohei Tateishi<sup>1</sup>, Ryuichi Itoi<sup>1</sup>, Toshiaki Tanaka<sup>1</sup>, Naoto Hiraga<sup>2</sup>, and Junichi Takayama<sup>2</sup>

<sup>1</sup>Department of Earth Resources Engineering,  
Faculty of Engineering, Kyushu University, Fukuoka, Japan  
<sup>2</sup>Nittetsu Mining Co., Ltd., Tokyo, Japan

## Keywords

Ogiri, Ginyu fault, numerical model, steam-water two-phase zone, MINC method

## ABSTRACT

Numerical simulations of the Ogiri geothermal reservoir were conducted using a fractured reservoir model with particular focus on the periods of power plant maintenance when all production and reinjection wells are shut-in for a few weeks. The results show that the steam-water two-phase zone in the shallow reservoir shrinks somewhat and the single-phase water zone expands.

## Introduction

The Ogiri geothermal field is located in Kagoshima prefecture, southern Kyushu, Japan. The Ogiri geothermal power plant started operating in March 1996 with an installed capacity of 30 MW. The reservoir lies along the Ginyu fault, the main geologic feature of the field. In the Ogiri geothermal field, a steam-water mixture is produced from a fractured reservoir in the Ginyu fault zone. Separated hot water is reinjected back into the reservoir in the western part of the field to maintain reservoir pressure. Pressure drawdown in the reservoir due to production operations has caused the formation of a steam-water two-phase zone in the shallow part of reservoir. Shallow wells produce dry steam whereas deeper wells produce a steam-water two-phase mixture.

Every two years, the Ogiri geothermal project shuts in all production and reinjection wells for periodic inspection of the plant. This causes a reduction in the vertical extent of the two-phase region in the shallow part of the reservoir as well as partial pressure recovery in the deeper part of the reservoir. When pro-

duction and reinjection operations resume, the two-phase region appears to re-expand. These temporary field shutdowns generally cause changes in pressure and phase conditions in the reservoir. Therefore, understanding the recovery of the two-phase zone when the wells are restarted at the end of the inspection period is important for designing restart procedures for the shallow wells.

Reservoir modeling and numerical simulations of reservoir performance at Ogiri have been carried out by Kumamoto et al. (2008, 2009), Yamashita et al. (2009, 2011) and Itoi et al. (2010). They conducted a series of simulations to reproduce the natural state of the reservoir and to carry out post-1996 history matching with a three dimensional numerical model using the TOUGH2 simulator (Pruess et al 1999). We improved their model and analyzed the behavior of the pressure recovery in observation well KE1-19S and the phase changes in the shallow reservoir with time upon shutin and subsequent restart of the production/reinjection wells at the time of the 2009 power plant inspection. The production and reinjection zones in the Ginyu fault were treated using

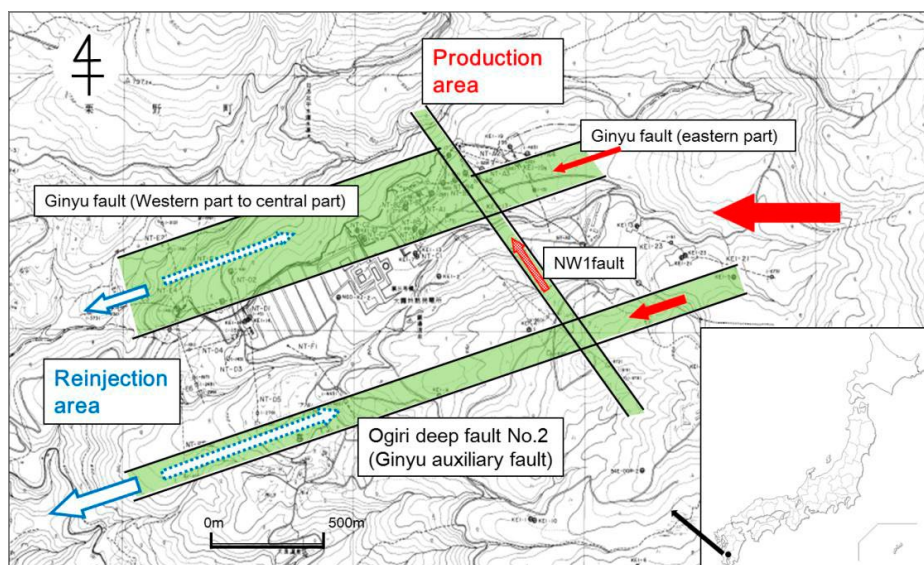


**Figure 1.** Conceptual model of the Ogiri geothermal field. Red and blue arrows denote estimated flow directions of high temperature fluid from heat source and reinjected water, respectively.

the MINC method while more distant parts of the system were represented as ordinary porous media.

### Characteristics of the Ogiri Field

The pre-exploitation Ogiri subsurface temperature distribution features a high temperature zone in the eastern part of the field with temperature gradually decreasing to the west. This implies that the heat source charging the area lies to the south-east of Ogiri, below the Kirishima volcanoes. The Ogiri geothermal reservoir is characterized by a fault system that includes the Ginyu fault, the Ogiri deep fault No.2 and the NW1 fault. The ENE-WSW Ginyu fault is the main reservoir for steam production, with temperatures around 230°C. There is a low permeability cap rock in the shallow area of this reservoir below which is found a two-phase zone. Because of the high permeability of the Ginyu fault and the presence of the steam-water two-phase zone, production wells were drilled mainly along the Ginyu fault. The Ogiri deep fault No.2 is located parallel to the Ginyu fault, to the south. Its temperature is estimated to be between 220 and 240°C (Goko, 2004). This implies that this deep fault could also be productive. The NW1 fault strikes NW to SE and intersects both the Ginyu fault and the Ogiri deep fault No.2. Therefore, the NW1 fault may serve as a flow path for high temperature fluids between the Ginyu fault and the Ogiri deep fault No.2. Figure 1 shows a schematic model of Ogiri with flow directions of high temperature fluids and reinjected water, and locations of main faults.

The basement rock in the Kirishima area is the Shimanto group. This basement rock is unconformably overlain by volcanic rocks and lacustrine sediment deposits. The feedzones of the production and injection wells are hosted by the deep Makizono lava formation. A low permeability layer forms the shallow cap rock.

### Three Dimensional Numerical Model

Ogiri is a fracture-dominated geothermal reservoir. The MINC method is useful for describing such systems in numerical models. We began by improving the three dimensional model developed by Yamashita et al. (2011), which only applied MINC to grid blocks within the production and reinjection areas of the Ginyu Fault. Since the reinjected water is reheated through the Ogiri deep fault No.2, this implies that the Ogiri deep fault No.2 and the NW1 fault should also incorporate MINC fracture modeling. Our improved three-dimensional grid system covers an area of 5.5 km x 3.9 km between elevations of 230 m a.s.l down to 2600 m b.s.l. The grid block size varies from 100 m x 100 m to 1000 m x 1000 m and the thickness of the vertical layers ranges from 30 m to 1600 m. The east-west extent of the grid system is divided into 23 blocks and the north-south extent into 12 blocks. Depth is divided into 14 layers, named from A to N from top to bottom. The total number of grid blocks in the numerical model is 3864.

In this geometry, the MINC model is applied to the production zone of the Ginyu fault, the Ogiri deep fault No.2 and the NW1 fault. Using the MINC model, each macroscopic grid block is subdivided into three parts (*Fracture, Matrix1* and *Matrix2*), with volume ratios of 4%, 20% and 76%, respectively. For the *Matrix* sub-blocks, rock permeability of  $10^{-17}m^2$  and porosity of 10% are assigned. The *Fracture* sub-blocks are assigned 50% porosity and 25 m fracture spacing. Other blocks are treated as porous media. Thirteen different rock types are used in the numerical model. Figure 2 shows the rock type assignments in Layers A to N; these assignments reflect the known geological and hydrogeological characteristics of the Ogiri geothermal system as closely as possible. Thermal conductivities of the rock types range from 1.5 to 3.0 W/m°C. Porosity (10%), density (2500 kg/m<sup>3</sup>) and specific heat (1050 J/kg°C) are the same for all rock types. (Kumamoto et al., 2008).

Figure 3 shows feedzone locations of production, reinjection, observation and exploration wells in plan view relative to the grid. For history matching, we imposed the known well histories of production and reinjection rate as input data. These flowrates were assigned as mass sinks and sources in the grid blocks containing the feedzones.

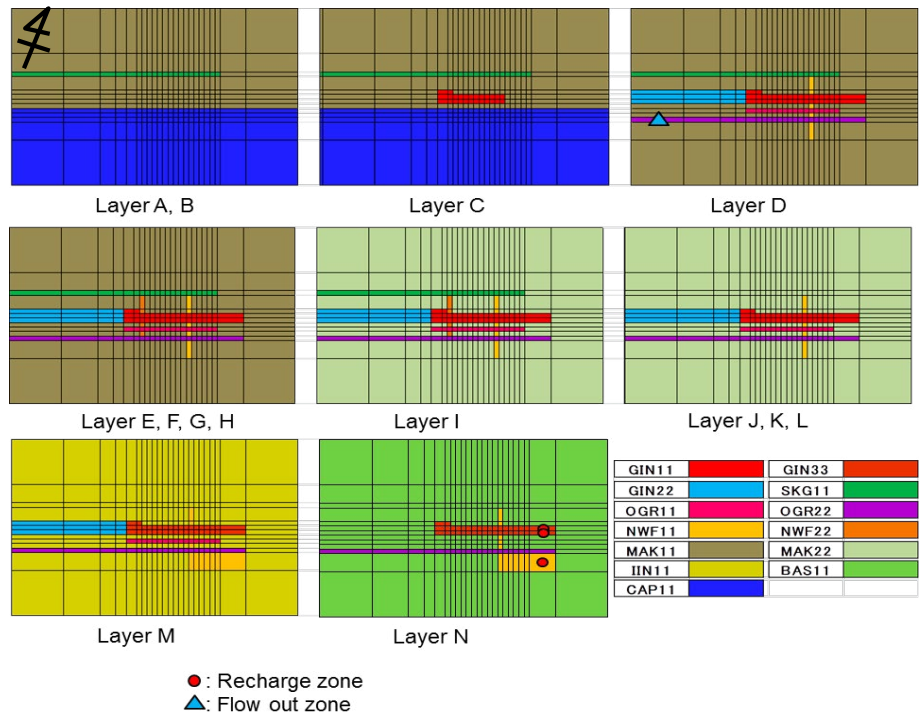
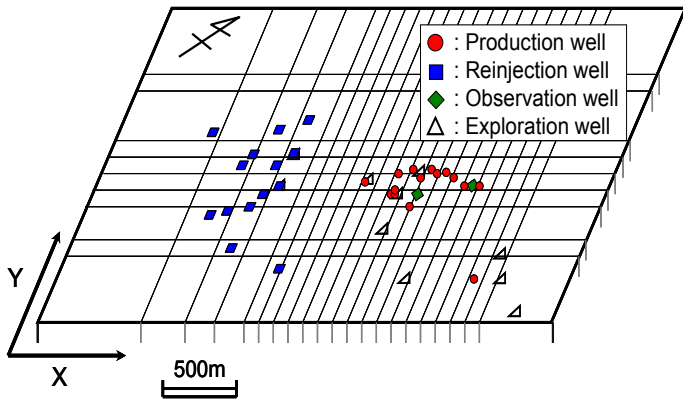


Figure 2. Assignment of rock types in Layer A to Layer N.

### Natural State Simulation

#### Simulation Conditions

We developed the numerical model using the TOUGH2 numerical simulator. Firstly, we carried out a natural-state simulation to obtain the temperature and pressure distributions in the Ogiri geothermal area before exploitation. In the natural-state simulation, we compared simulated results with measured temperatures in 15 wells and measured pressure values at the feedpoints of 10



**Figure 3.** Feedzone locations of production, reinjection, observation and exploration wells in plan view of numerical model.

wells. The forward simulation was repeated until rough matches were obtained between measured and simulated values.

For initial conditions for the natural-state simulation, a pressure equilibrium condition saturated with water at 75°C was specified in each grid block. For boundary conditions, an infinitely large block filled with water at pressure  $9.804 \times 10^4$  Pa and temperature 75°C was assigned above the top of the grid model. The lateral boundaries of the model were impermeable to mass and adiabatic to heat. However, there was an outflow of fluid allocated in the western shallow zone of the Ogiri deep fault No.2 indicated by a blue triangle in Fig.2. The outflow rate was calculated by using a productivity index (PI) of  $0.75 \times 10^{-11}$  m<sup>3</sup>. This value was determined by trial and error during the simulations. High temperature 230°C mass recharge with total flowrate 45 kg/s was specified at two locations in the bottom layer indicated as solid circles in Fig.2. Two values of conductive heat flux were also prescribed at the bottom of the model: 0.35 W/m<sup>2</sup> in the bottom layer in the south-east part of the numerical model and 0.23 W/m<sup>2</sup> in the remaining area.

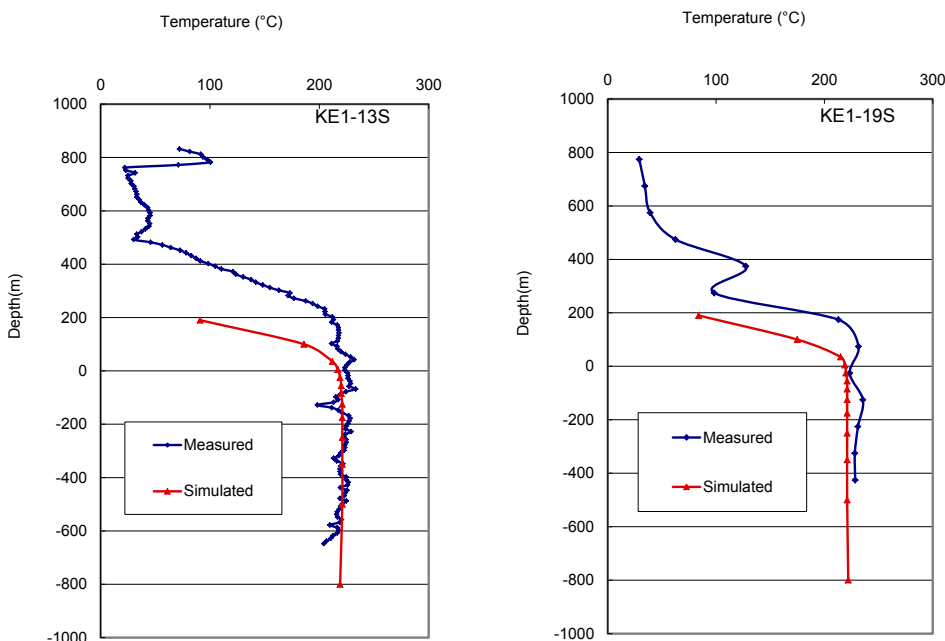


**Figure 4.** Comparison between measured and simulated temperature values of observation wells during natural-state simulation.

## Results

Figure 4 presents the comparison between measured and simulated natural-state temperature profiles for two observation wells, KE1-13S and KE1-19S, located in the Ginyu fault. The simulated temperature of Well KE1-13S is too low at shallow depths but exhibits a reasonable match at deeper levels. On the other hand, the computed temperature values in Well KE1-19S at all depths seem to be shifted about 10°C below the measured values. Figure 5 shows the results of comparisons between measured and simulated pressure values. These figures indicate reasonable natural-state simulation matches.

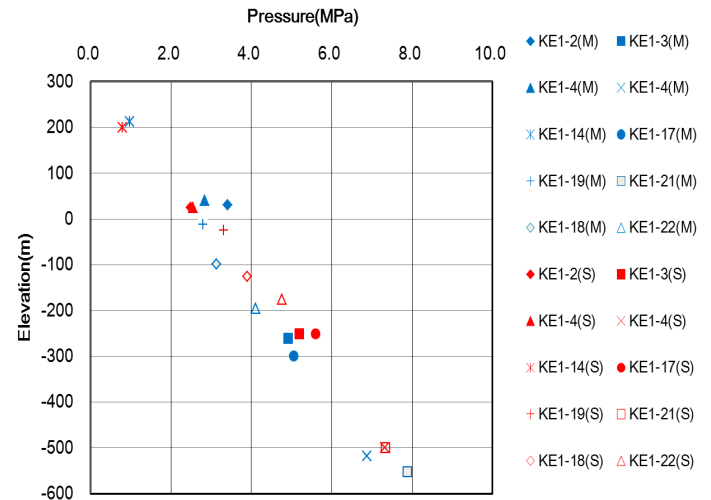


**Figure 5.** Comparison between measured (M) and simulated (S) well feed-point pressure values for natural-state simulation.

## Production and ReInjection Simulation Simulation Conditions

In order to reproduce the reservoir conditions before the 2009 power plant maintenance shutdown, numerical simulations were conducted using simplified production and reinjection well flow histories starting in 1996. Production and reinjection rates as of 2009 for 12 production wells and 5 reinjection wells were specified for 13 years from 1996 until 2009. Temperature and pressure distributions obtained from the natural-state simulation were prescribed as initial conditions for these simulations.

Boundary conditions were the same as for the natural state simulation. In this simulation, relative permeabilities were represented by Corey's curves for the porous-medium part of the grid and linear functions for the fractured region. Residual saturations of 0.3 and 0.05 for water and steam, respectively, were specified for both relative permeability curves (Pruess, 1985).

Figure 6 shows the measured and simulated values of pressure in Well KE1-19S

with time. Occasional spikes in the measured pressure history occur when periodic inspection of the power plant took place. The match between the measured and the simulated pressure values is relatively good throughout the simulation period. Figure 7 shows the comparison between measured and simulated enthalpy values for production well A2. The figure shows a reasonable enthalpy match. The simulated results after 13 years of production and reinjection were then provided as initial conditions for the subsequent simulation to analyze the pressure and steam-water two-phase zone transients when the wellfield was shut in for the scheduled maintenance operations and then restarted .

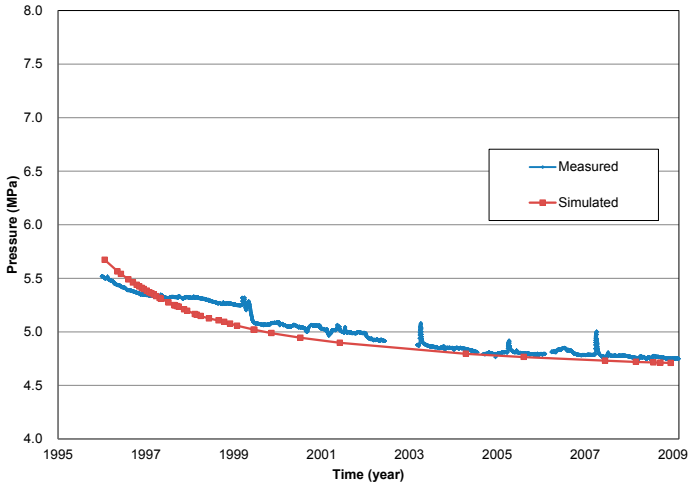


Figure 6. Measured and simulated pressures in Well KE1-19S.

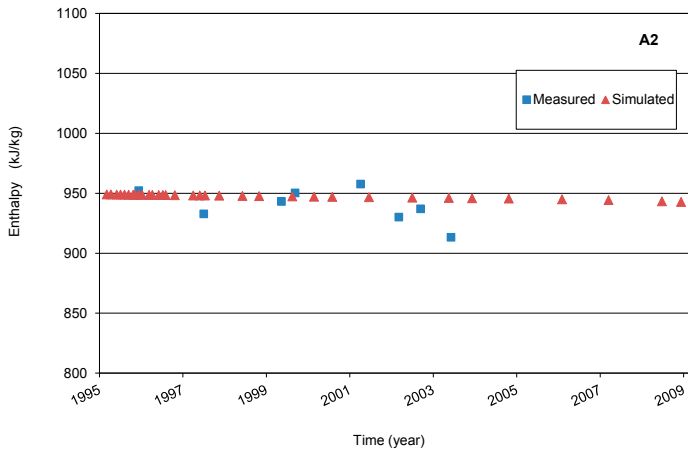


Figure 7. Comparison between measured and simulated enthalpy value of Well A2.

### Effects of Relative Permeability Curves

We examined the effects of the relative permeability curves on pressure recovery during the maintenance period. Two combinations of relative permeability curves were applied: CASE1 with Corey’s curves for the porous region and Grant’s curves for the fractured region, and CASE2 with Corey’s curves for the porous region and linear curves for the fractured region. The residual saturation values of 0.3 and 0.05 for water and steam respectively were maintained in both cases. Thirteen years of simulation from

1996 to 2009 was conducted for these two cases, then the simulation was carried forward into the subsequent shut-in/restart period including pressure recovery and drawdown. Figure 8 shows the pressure recovery in Well KE1-19S for the two cases. This observation well represents the reservoir pressure in the single phase water zone at a depth of 400 m b.s.l. The horizontal axis denotes time since the halt of production and reinjection operations. Pressures at zero time are slightly different between the two cases. The pressure recovery of CASE1 shows a linear increase with time whereas that of CASE2 shows a rapid pressure increase at early times, then more gradual recovery. It appears that the CASE2 relative permeability representation gives a better pressure recovery match than CASE1. Therefore, we used the CASE2 relative permeabilities for the subsequent simulations.

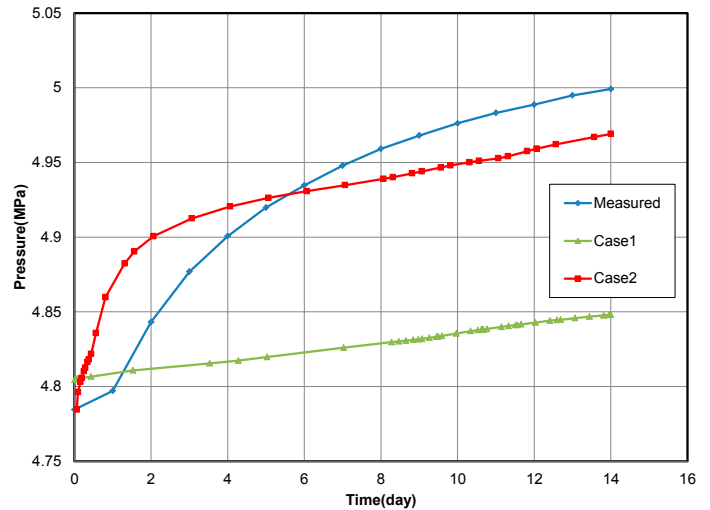


Figure 8. Effects of relative permeability curves on pressure recovery in Well KE1-19S.

We next adjusted the permeabilities of the deep Ginyu fault (rock types GIN11, GIN22, and GIN33) in the model as shown in Table 1. Figure 9 shows the comparison of pressure recovery and drawdown in Well KE1-19S for these four runs with different deep Ginyu fault permeabilities. The results show that the lowest permeability considered causes the pressure to increase rapidly with time and discrepancies between the measured and simulated pressures increase with time in that case. The results for RUN3 show the best match with the measured pressure recovery and drawdown. Thus, the results of RUN3 were examined to evaluate the spatial extent of the two-phase zone in the Ginyu fault zone.

Table 1. Permeability of rock types GIN11, GIN22, and GIN33 for the deep Ginyu fault.

	$k_x, k_y (m^2)$	$k_z (m^2)$
<b>RUN1</b>	$1.00 \times 10^{-14}$	$2.00 \times 10^{-14}$
<b>RUN2</b>	$3.16 \times 10^{-15}$	$6.32 \times 10^{-14}$
<b>RUN3</b>	$1.20 \times 10^{-15}$	$2.00 \times 10^{-15}$
<b>RUN4</b>	$3.16 \times 10^{-16}$	$6.32 \times 10^{-15}$

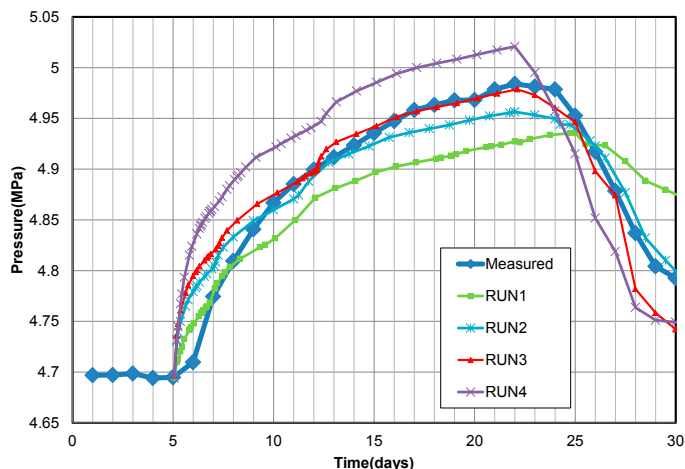


Figure 9. Pressure recovery/drawdown in Well KE1-19S for RUN1, RUN2, RUN3 and RUN4.

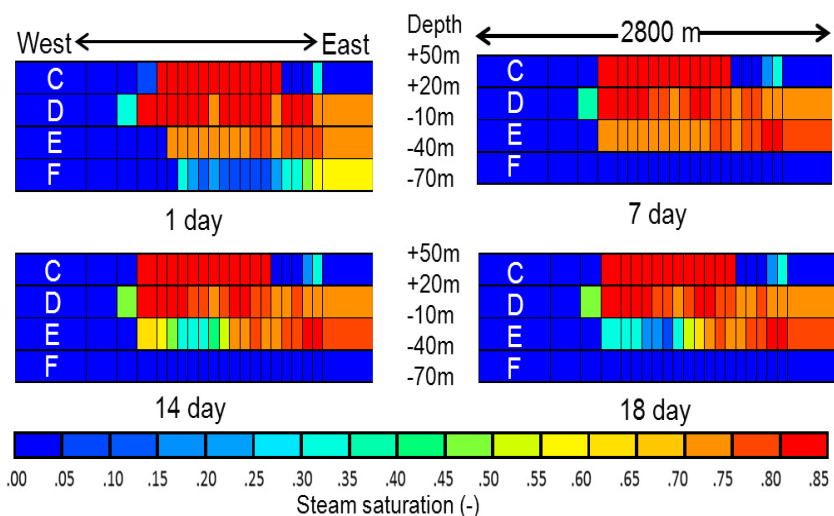


Figure 10. Distribution of steam saturation with time in the cross section of the Ginyu fault for Layers C to F after production and reinjection operations ceased.

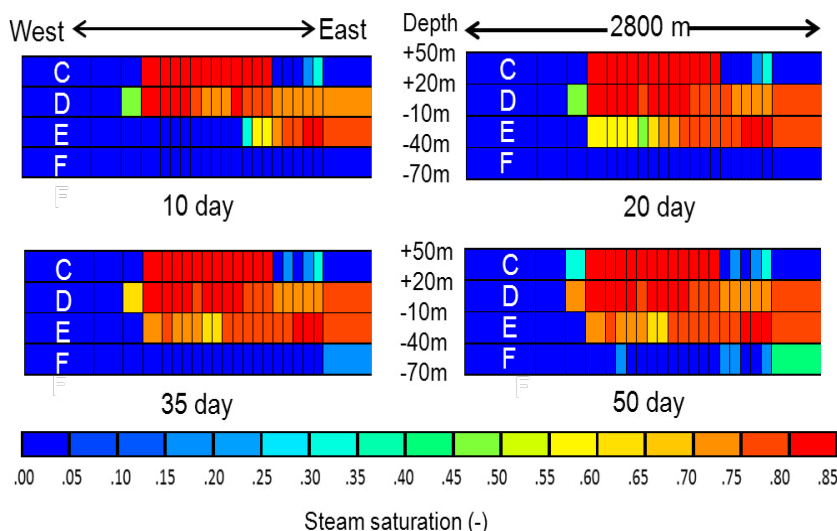


Figure 11. Simulated steam saturation distribution in the cross section of the Ginyu fault for Layers C to F after the restart of production and reinjection operations.

Figure 10 shows the changes in the steam saturation distribution with time in the cross section of the Ginyu fault in Layers C to F after the wells were shut in. These layers correspond to the depths from +50 m down to -70 m where the feedzones of the shallow production wells are located. Within 7 days after shut-in, steam saturations decrease in Layer F, then the layer becomes single-phase water. In shallow layers C, D and E, the two-phase zone persists without any significant change in steam saturation during this period. However, after 14 days, the steam saturations in the western area of Layer E decreases. This is probably because liquid water flows upward from the deep zone into the steam-water two-phase zone. Then, the steam saturation in the western part of Layer E gradually decreases with time whereas that in Layers C and D remains the same.

Figure 11 shows the simulated steam saturation distribution results with time in Layers C to F after production and reinjection operation resume. To the west, Layer E remains mostly single phase water even 10 days after restart. The phase change caused by the shut-in during the pressure recovery period still persists. The steam-water two-phase zone in Layer E, however, expands toward the west as shown in the figure after 20 days, and its saturation value increases to the east. It seems that more time is required to re-form the steam-water two-phase zone in Layer F as the steam saturation in Layer F remains small even after 50days.

## Conclusions

We carried out numerical simulations of the Ogiri geothermal reservoir with an improved numerical model to examine pressure recovery and phase changes caused by the shut-in of production and reinjection wells for plant maintenance. Results are summarized as follows:

1. A good match for the pressure recovery in an observation well was obtained using linear relative permeability curves for fractured regions and Corey's curves elsewhere.
2. The simulated results indicate that steam-water two-phase conditions in the lower part of shallow reservoir disappear during the well shut-in period. The two-phase zone in the shallowest part of the shallow reservoir persists throughout the plant maintenance period in spite of well shut-in and restart.

## Acknowledgement

The authors would like to thank Nittetsu Mining Co., Ltd. for their support and for permission to use their data.

## References

Goko, K., *Towards Sustainable Steam Production; the Example of the Ogiri Geothermal Field*, Journal of the Geothermal Research Society of Japan (in Japanese with English abstract), 26, pp.151-164 (2004).

- Bodvarsson, G. S., Pruess, K., O'Sullivan, M. J., "Injection and Energy Recovery in Fractured Geothermal Reservoirs", SPE Journal, April., p303-310 (1985).
- Itoi, R., Kumamoto, Y., Tanaka, T. and Takayama, J., "History Matching Simulation of the Ogiri Geothermal Field, Japan", Proc. World Geothermal Congress 2010, Bali, Indonesia, p.25-29 (2010).
- Kumamoto, Y., Itoi, R., Horne, R. and Hazama, Y., "Numerical Modeling of the Ogiri geothermal system, Kyushu, Japan", Trans. Geothermal Resources Council, **32**, p.449-458(2008).
- Kumamoto, Y., Itoi, R., Tanaka, T., and Hazama, Y., "Modeling and Numerical Analysis of the Two-phase Geothermal Reservoir at Ogiri, Kyushu, Japan", Proc. 34th Workshop on Geothermal Reservoir Engineering, Stanford University, Stanford, CA(2009).
- Pruess, K., C. Oldenburg, and G. Moridis., "TOUGH2 User's Guide, Version 2.0." Report LBNL-43134, Earth Sciences Division, Lawrence Berkeley National Laboratory, University of California, Berkeley, California (1999).
- Yamashita S., R. Itoi, and T. Tanaka, "A Three dimensional numerical modeling of the Ogiri geothermal system using TOUGH2 and iTOUGH2.", International Symposium on Earth Science and Technology, p.523-528(2011).